Received: 1 June 2023 | Revised: 10 November 2023 | Accepted: 13 November 2023

DOI: 10.1002/jbm.a.37651

RESEARCH ARTICLE

Society For Biomaterials WILEY

# Varying the RGD concentration on a hyaluronic acid hydrogel influences dormancy versus proliferation in brain metastatic breast cancer cells

Kasra Goodarzi | Rachel Lane | Shreyas S. Rao

Department of Chemical and Biological Engineering, The University of Alabama, Tuscaloosa, Alabama, USA

**Correspondence**
Shreyas S. Rao, Department of Chemical and Biological Engineering, The University of Alabama, Tuscaloosa, AL 35487-0203, USA.
Email: srao3@eng.ua.edu

**Funding information**
National Science Foundation, Grant/Award Number: CBET 1749837; Alabama EPSCoR Graduate Research Fellowship

## Abstract

A majority of breast cancer deaths occur due to metastasis of cancer cells to distant organs. In particular, brain metastasis is very aggressive with an extremely low survival rate. Breast cancer cells that metastasize to the brain can enter a state of dormancy, which allows them to evade death. The brain microenvironment provides biophysical, biochemical, and cellular cues, and plays an important role in determining the fate of dormant cancer cells. However, how these cues influence dormancy remains poorly understood. Herein, we employed hyaluronic acid (HA) hydrogels with a stiffness of ~0.4 kPa as an in vitro biomimetic platform to investigate the impact of biochemical cues, specifically alterations in RGD concentration, on dormancy versus proliferation in MDA-MB-231Br brain metastatic breast cancer cells. We applied varying concentrations of RGD peptide (0, 1, 2, or 4 mg/mL) to HA hydrogel surfaces and confirmed varying degrees of surface functionalization using a fluorescently labeled RGD peptide. Post functionalization, ~10,000 MDA-MB-231Br cells were seeded on top of the hydrogels and cultured for 5 days. We found that an increase in RGD concentration led to changes in cell morphology, with cells transitioning from a rounded to spindle-like morphology as well as an increase in cell spreading area. Also, an increase in RGD concentration resulted in an increase in cell proliferation. Cellular dormancy was assessed using the ratio of phosphorylated extracellular signal-regulated kinase 1/2 (p-ERK) to phosphorylated p38 (p-p38) positivity, which was significantly lower in hydrogels without RGD and in hydrogels with lowest RGD concentration compared to hydrogels functionalized with higher RGD concentration. We also demonstrated that the HA hydrogel-induced cellular dormancy was reversible. Finally, we demonstrated the involvement of β1 integrin in mediating cell phenotype in our hydrogel platform. Overall, our results provide insight into the role of biochemical cues in regulating dormancy versus proliferation in brain metastatic breast cancer cells.

**KEYWORDS**
dormancy, hyaluronic acid, hydrogel, metastasis

## 1 | INTRODUCTION

Breast cancer is the most common form of cancer in women worldwide, accounting for 25% of all cancer cases in women.[1,2] In 2020, there were over 2.3 million newly diagnosed instances and 685,000 deaths of breast cancer, that is 1 out of 6 cancer deaths in women.[3,4] A majority of deaths from breast cancer occur because of metastasis to distant organs. Metastatic breast cancer is the second most common solid tumor to induce brain metastases, behind lung cancer.[5–7] To thrive in the brain, metastatic breast cancer cells must acquire a specific set of traits that enable them to traverse the blood–brain barrier, initiate neoangiogenesis, and start growing with perivascular proliferation.[5–7] In addition, these cancer cells are able to stay in a dormant state for extended periods of time and later outgrow into metastasis.[8–11] The inability to fully comprehend the mechanisms associated with breast cancer brain metastasis (BCBM), particularly, control of the dormant state, prevents the development of effective therapeutic strategies for BCBM.

Steven Paget's "seed and soil" hypothesis suggests that the ability of cancer cells to metastasize and grow at distant tissues is linked to both the cancer cells' innate features (seed) and the availability of a favorable microenvironment (soil).[12,13] The brain microenvironment presents multiple cues (i.e., biophysical, biochemical, and cellular cues) to cancer cells and plays an important role in determining the fate of cancer cells, including control of the dormant state. However, studying the contributions of these cues in regulating tumor cell dormancy using in vivo mouse models is challenging, as they provide limited control of the local microenvironment. Furthermore, animal–animal variation, as well as high costs, makes it difficult to study the contribution of these cues in regulating tumor cell dormancy.

Recently, biomaterial-based culture platforms have emerged as an important tool to study regulation of the dormant state in vitro.[14,15] For example, natural biomaterials, including hyaluronic acid (HA),[16] Collagen I,[17] Matrigel,[18] and Fibrin,[19] as well as synthetic biomaterials such as polyethylene glycol (PEG)-based hydrogels[20,21] have been employed to study microenvironmental regulation of dormancy in vitro. In the context of BCBM, we previously reported a biomimetic HA hydrogel-based in vitro platform to study regulation of the dormant state mediated by biophysical cues in brain metastatic breast cancer cells.[22] Specifically, we found that cells cultured on soft (∼0.4 kPa) versus stiff (∼4.5 kPa) HA hydrogels functionalized with identical levels of RGD peptide exhibited a dormant versus proliferative state. However, the impact of varying RGD peptide concentration on the regulation of dormancy versus proliferation in this culture platform was not investigated.

To bridge this gap, in this study, we employed HA hydrogels with a stiffness of ∼0.4 kPa to mimic the brain extracellular matrix and functionalized them with various concentrations of integrin binding peptide (RGD). We confirmed varying degrees of surface functionalization using a fluorescently labeled RGD peptide. Post functionalization, we seeded MDA-MB-231Br brain metastatic breast cancer cells on top of HA hydrogels with varying RGD concentrations and investigated how these environments influence cell adhesion, morphology, spreading, as well as dormancy versus proliferation. Finally, we tested reversibility of the dormant phenotype and the involvement of integrin β1 via blocking studies.

## 2 | MATERIALS AND METHODS

### 2.1 | HA hydrogel preparation

Hyaluronic acid methacrylate (HAMA) was synthesized using a previously established procedure.[22,23] Briefly, a 1 wt% HA (66–90 kDa; Lifecore Biomedical) aqueous prepolymer solution was prepared overnight. HA solution was methacrylated by reacting with ∼18-fold molar excess of methacrylic anhydride (Sigma Aldrich) at 4°C while pH was maintained between 8 and 10 using 5 M NaOH solution. A fivefold volumetric excess of cold acetone was added to the final solution to extract HAMA, which was frozen and freeze-dried overnight. In this study, we used HAMA with ∼85% methacrylation degree as specified by proton nuclear magnetic resonance ($^1$H NMR). To fabricate HA hydrogels, a gel precursor solution containing 5 wt% HAMA in serum-free Dulbecco's modified eagle's medium (DMEM; Sigma Aldrich) was prepared. Then, crosslinker Dithiothreitol (DTT; Sigma Aldrich) was added to the hydrogel precursor solution at a final concentration of 10 mM. Next, 75 μL of this solution was added to each well of a 96-well plate, and the plate was incubated at 37°C overnight. This formulation yields ∼0.4 kPa HA hydrogels as measured through compression testing performed on RSA-G2 solid analyzer instrument (TA Instruments). To fabricate HA hydrogels with various cell adhesion sites, the hydrogel surfaces were functionalized with different concentrations of the integrin binding peptide (RGD) with GCGYGRGDSPG sequence (GenScript). Briefly, in serum-free DMEM, we prepared RGD solutions at concentrations of 0, 1, 2, or 4 mg/mL. Following that, we applied 25 μL of the RGD solution to the surface of HA hydrogels. The hydrogels were then incubated at room temperature for 3 h to allow for the thiol-Michael addition reaction between the methacrylated functional groups on the HAMA backbone and the thiol group of the cystine amino acid (C) in the RGD sequence. This results in the covalent attachment of RGD peptides to the hydrogel surface, providing cells with adhesive sites. Following the 3 h incubation period, the hydrogels were thoroughly washed three times with serum-free DMEM to remove any unreacted or physically attached RGD peptides from the hydrogel surface, leaving only chemically bound RGD.

### 2.2 | Quantification of attached RGD to the HA hydrogel

To quantify the amount of RGD attached to the hydrogel, HA hydrogels were prepared using PBS instead of DMEM. After the hydrogels were prepared using the aforementioned method, 25 μL of RGD solution containing 5% fluorescently labeled RGD peptide (sequence: GCGYGRGDSPG) (GenScript) with similar total concentrations (0, 1,

2, and 4 mg/mL) were applied to the surface of HA hydrogels. The functionalized hydrogels were then incubated for 3 h at room temperature. Subsequently, the functionalized hydrogels were washed with PBS three times to eliminate any unreacted fluorescently labeled RGD and the fluorescence was read using a FilterMax F5 multi-mode microplate reader. To determine the concentration of RGD attached to the HA hydrogels, a standard curve was prepared using known concentrations of fluorescently labeled RGD in PBS and total functionalized RGD concentration for each condition was calculated based on the functionalization of 5% fluorescently labeled RGD.

## 2.3 | Cell culture

In this study, we used MDA-MB-231Br cells, a brain metastasizing variant of the triple-negative breast cancer line MDA-MB-231 (generously provided by Dr. Lonnie Shea [University of Michigan]). MDA-MB-231Br cells were cultured in DMEM (Sigma Aldrich) supplemented with 10% fetal bovine serum (FBS; VWR Life Science) and 1% penicillin–streptomycin in a 37°C and 5% $CO_2$ environment. The cells were passaged at ~80% confluency and were then seeded onto the hydrogel surface.

## 2.4 | Optical imaging, cell adhesion, and single cell area measurements

To assess short term cell adhesion as function of varying RGD concentration, ~10,000 MDA-MB-231Br cells were seeded onto hydrogel surfaces and allowed to incubate for a duration of 1.5 h. The media was then removed from the wells, followed by a light wash using 1× phosphate-buffered saline (PBS) (Gibco), and fresh media was added. Subsequently, the wells were imaged using a bright field microscope in order to determine the number of cells present per field of view.

To evaluate the impact of varying RGD concentration on cell spreading, 10,000 MDA-MB-231Br cells were seeded onto HA hydrogels and imaged using an Olympus IX83 microscope equipped with a spinning disk confocal attachment. Images of the cells were captured within 30 min of seeding on day 0 and at day 5 post cell seeding. The area of each individual cell was measured using Image-J software, following a manual selection of the cell boundary as previously described.[23] Atleast 12 images per condition were analyzed.

## 2.5 | Cell viability

To qualitatively assess cell viability, we stained cells with Calcein AM (Thermo Fisher Scientific) as described previously.[24] Briefly, on day 5, cell seeded hydrogels were incubated in 100 µL of fresh media containing $4 \times 10^{-6}$ M Calcein AM for 1 h at 37°C and 5% $CO_2$. The samples were then washed in PBS (Gibco). Fluorescence images were obtained using an Olympus IX83 microscope with a spinning disk confocal attachment.

## 2.6 | EdU cell proliferation assay

To measure the proliferation of MDA-MB-231Br cells on HA hydrogels, we used the Click-iT™ EdU Cell Proliferation Kit (Thermo Fisher Scientific) as described in prior studies.[25,26] In brief, 10,000 MDA-MB-231Br cells were seeded on HA hydrogels with varying RGD concentrations. After 4 days in culture, 10 µM EdU was added to the cell culture media on each HA hydrogel and incubated with the cells overnight. On day 5, the EdU-containing media was discarded, and the cells were trypsinized for ~5 min before being retrieved from the HA hydrogels. The cells were then transferred to a 96-well plate and 100 µL of 4% paraformaldehyde was added to fix the cells at room temperature (RT) for 20 min. Next, 100 µL of a 0.25% Triton-X solution was added to the cells for 15 min at RT to permeabilize them. The cells were then blocked with 100 µL of a 5% bovine serum albumin (BSA) solution at 4°C for 30 min following which they were incubated with the reaction cocktail prepared according to the manufacturer's instructions, for 30 min in the dark at RT. The cell nuclei were stained at RT with 4,6-diamidino-2-phenylindole (DAPI) (Invitrogen). The cells were washed with PBS between each step, and the plate was centrifuged for 1 min at 1000*g* to settle cells at the bottom before any liquid was aspirated. Imaging was performed using an Olympus IX83 microscope with a spinning disk confocal attachment. EdU positive cells were manually counted using the multi-point tool in ImageJ software (NIH).

## 2.7 | Immunofluorescence staining

We performed immunofluorescence staining for p-ERK and p-p38, as these markers have been shown to be differentially expressed between proliferative and dormant cells in previous studies.[27,28] To determine the percentage of p-ERK and p-p38 positive cells on day 5, cells were gently trypsinized for ~5 min, allowing their detachment from the HA hydrogels. Subsequently, these cells were transferred to a 96-well plate, where they underwent fixation, permeabilization, and blocking, following the previously outlined procedures. For assessing p-ERK and p-p38 intensity, hydrogel constructs containing cells were directly subjected to the same fixation, permeabilization, and blocking procedures as described earlier. Next, the cells were incubated at 4°C overnight in primary antibody solution (p-ERK [Cell Signaling Technology, C#4370S—1:200]; p-p38 [Cell Signaling Technology, C#9216S—1:200]). On the following day, cells were fluorescently labeled by incubating them for 1 h at 4°C with secondary antibodies (goat anti-rabbit antibody, Thermo Fisher Scientific [A11034-1:1000] and goat anti-mouse antibody, Thermo Fisher Scientific [A11001-1:1000] for p-ERK and p-p38, respectively). Cells were then counter stained for DAPI. Imaging was performed using an Olympus IX83 microscope with a spinning disk confocal attachment. For each marker, all images were taken at the same exposure time. For quantifying percentage positive cells or mean fluorescence intensity of the images, Image J software was used. To adjust for background noise, intensity measurements of

five non-cell containing background regions were quantified and averaged for each image. The p-ERK and p-p38 intensity values were calculated by subtracting the average of background intensity data from the mean intensity of the image as described previously.[29] These values were then averaged for all images in each experimental condition. The intensity ratio for each condition was then calculated by taking the ratio of mean intensity of p-ERK to the mean intensity of p-p38.

### 2.8 | Integrin β1 blocking studies

For integrin β1 blocking studies, we seeded 10,000 MDA-MB-231Br cells on HA hydrogels functionalized with 4 mg/mL RGD solution. After 4 days, we added integrin β1 antibody (Santa Cruz Biotech) to the cell media, reaching a final concentration of 2 μg/mL. The cells were then incubated with the integrin β1 antibody for 24 h. Following this, we performed imaging to quantify cell spreading area. To evaluate cellular proliferation, we employed the Click-iT™ EdU Cell Proliferation Kit, as previously mentioned. Similarly, we evaluated cell spreading and cell proliferation post integrin β1 blocking (24 h) at day 12 post-transfer in studies investigating reversibility of the dormant phenotype.

### 2.9 | Statistical analysis

At least two independent experiments were conducted, each with at least two replicates. Unless otherwise specified, all numbers are presented as the mean ± standard deviation value. The PRISM software package was used for statistical analysis. To compare samples, Student's *t*-test or Brown-Forsythe ANOVA was run, with the method chosen depending on the number of data points. For comparison post ANOVA, Tukey-HSD test was used.

## 3 | RESULTS

### 3.1 | Quantification of RGD density on HA hydrogel surfaces

We quantified the RGD density on HA hydrogel surfaces using a fluorescently labeled RGD peptide. We generated a standard curve with known concentrations of fluorescently labeled RGD peptide in PBS (Figure S1) to determine the coating density of RGD on the surface of the hydrogels. Using this standard curve, we were able to determine the concentration of attached RGD to the HA hydrogels. Our findings indicate that the concentration of the applied RGD solution influences the amount of RGD attached to the HA hydrogel surface. As expected, a higher concentration of the applied RGD solution resulted in a greater amount of RGD attachment to the HA hydrogels (Table 1).

**TABLE 1** Quantification of functionalized RGD on HA hydrogel surfaces.

| Applied RGD solution concentration (mg/mL) | RGD coating density (μg/cm$^2$) |
|---|---|
| 4 | 140.8 ± 5.1 |
| 2 | 78.8 ± 7.3 |
| 1 | 35.2 ± 3.7 |
| 0 | 0 |

### 3.2 | MDA-MB-231Br cell adhesion, morphology, and spreading as a function of varying RGD concentration

We first examined MDA-MB-231Br cell adhesion, morphology, and spreading as a function of varying RGD concentration. We found that short term cell adhesion increased as a function of varying RGD concentration (Figure S2). We found that in the absence of RGD, cells exhibited a rounded morphology and were loosely attached to the hydrogel, possibly due to proteins adsorbing from the cell culture media. This rounded morphology was also observed in hydrogels with low RGD concentration, as opposed to spindle-shaped morphology noted at higher RGD concentration (Figure 1).

We also measured cell spreading area as a function of RGD concentration. We found that the concentration of functionalized RGD and cell spreading area were positively correlated (Figure 1).

In hydrogels without RGD, the average cell spreading area was 372 ± 103 μm$^2$. In hydrogels with applied RGD concentration of 1, 2, and 4 mg/mL, the cell spreading area was 702 ± 341 μm$^2$, 975 ± 778 μm$^2$, and 1204 ± 1136 μm$^2$, respectively. This was likely due to the increased number of possible cell attachment sites, supporting cell spreading. We also qualitatively assessed the viability of MDA-MB-231Br cells using Calcein AM staining. In all the conditions tested, cells adhered to the hydrogel surfaces were viable (Figure S3).

### 3.3 | MDA-MB-231Br cell proliferation as a function of varying RGD concentration

Next, we examined MDA-MB-231Br cell proliferation as a function of varying RGD concentration. We utilized EdU staining as EdU is frequently utilized as a marker to evaluate cancer cell proliferation and cell cycle progression.[30,31] EdU staining at day 5 revealed that the percentage of EdU positive cells was significantly lower in hydrogels without RGD and 1 mg/mL applied RGD concentration as opposed to hydrogels with 2 or 4 mg/mL applied RGD concentration.

Specifically, the percentage of EdU positive cells was 5.2% ± 6.8% in the absence of RGD, 5.3% ± 3.5% in the presence of 1 mg/mL applied RGD concentration, 18.3% ± 8.6% in the presence of 2 mg/mL applied RGD concentration, and 40.9% ± 14.4% in the presence of 4 mg/mL applied RGD concentration (Figure 2). These results

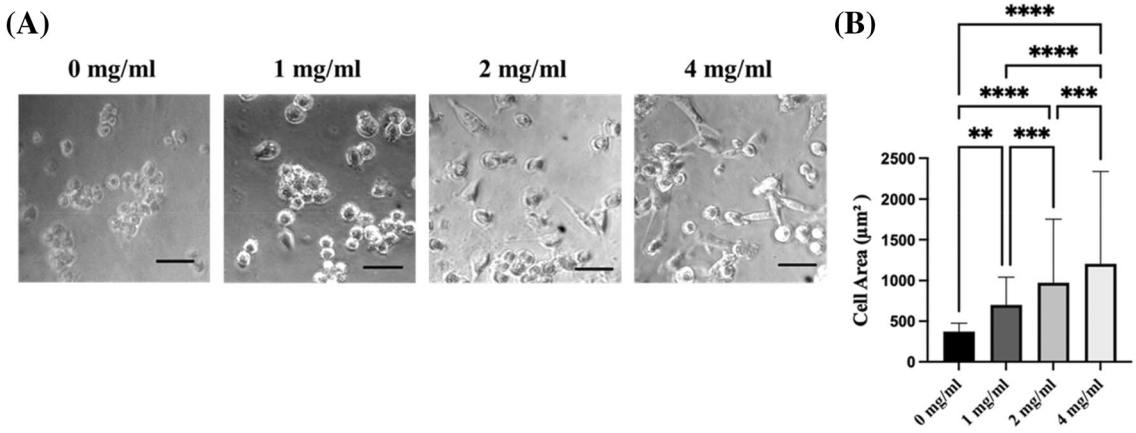


**FIGURE 1** Brain metastatic breast cancer cells cultured in the presence of higher concentrations of RGD adopt spindle-like morphology and a higher level of cell spreading. (A) Bright field images of day 5 of 10 k MDA-MB-231Br single cells seeded on HA hydrogels. (B) Quantification of cell spreading area as a function of the applied RGD concentration. Error bars represent standard deviations. Scale bar = 50 µm. $N \geq 4$ replicates per condition. Statistically significant difference indicator via Brown-Forsythe ANOVA followed by Tukey-HSD test: (**$p < .01$; ***$p < 0.001$; ****$p < .0001$).

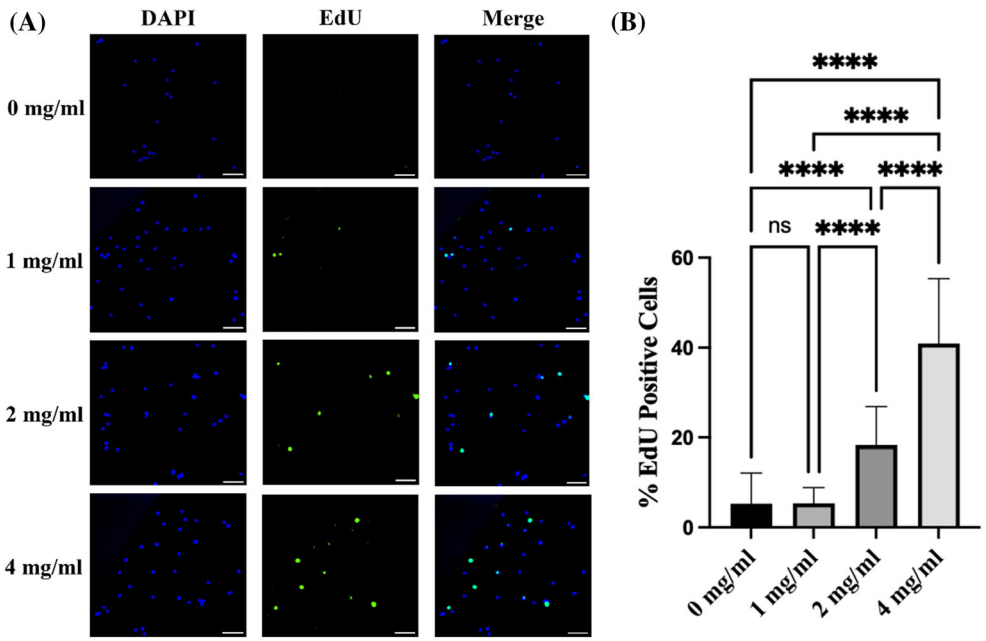


**FIGURE 2** Percentage of EdU-positive MDA-MB-231Br cells increase with an increase in applied RGD concentration on HA hydrogels. (A) Representative fluorescence microscopy images of EdU staining on day 5 of MDA-MB-231Br cells. (B) Quantification of EdU-positive MDA-MB-231Br cells cultured on HA hydrogels functionalized with various concentrations of RGD. Error bars represent standard deviation. Scale bar = 100 µm. $N \geq 5$ replicates per condition. Statistically significant difference indicator via Brown-Forsythe ANOVA followed by Tukey-HSD test (****$p < .0001$).

indicated that cells exhibited a proliferative phenotype on hydrogels with higher RGD concentration as opposed to those with lower RGD concentration or the absence of RGD, wherein the cells exhibited a dormant phenotype. The observed increase in cell proliferation also correlated with the cell spreading area measurements (Figure 1).

### 3.4 | Percentage of p-ERK and p-p38 positive cells as a function of varying RGD concentration

To further examine dormancy versus proliferation, we performed immunostaining for p-ERK and p-p38. The ERK signaling pathway plays a crucial role in facilitating the progression of cell cycle and promoting tumor growth. Further, it has been established that the activation of p38 signaling pathway induces cell-cycle arrest in tumor cells, promoting their survival.[32,33] Also, lower ratio of p-ERK to p-p38 has been reported to be an indicator of dormancy.[34]

The expression levels of phosphorylated ERK and p38 were assessed in MDA-MB-231Br cells via immunostaining on day 5 and quantified by percentage of positive cells. We found that the percentage of p-ERK positive cells was the highest in HA hydrogels with 4 mg/mL applied RGD concentration. In particular, HA hydrogels with 4 mg/mL applied RGD concentration exhibited a percentage p-ERK cell positivity of 45.2% ± 4.7%, whereas the percentage of p-ERK positive cells lowered to 32.2% ± 4.4%, 20.8% ± 5.7%, and 14.1% ± 3.1%, respectively, for conditions with 2, 1, and 0 mg/mL of applied RGD concentration, respectively

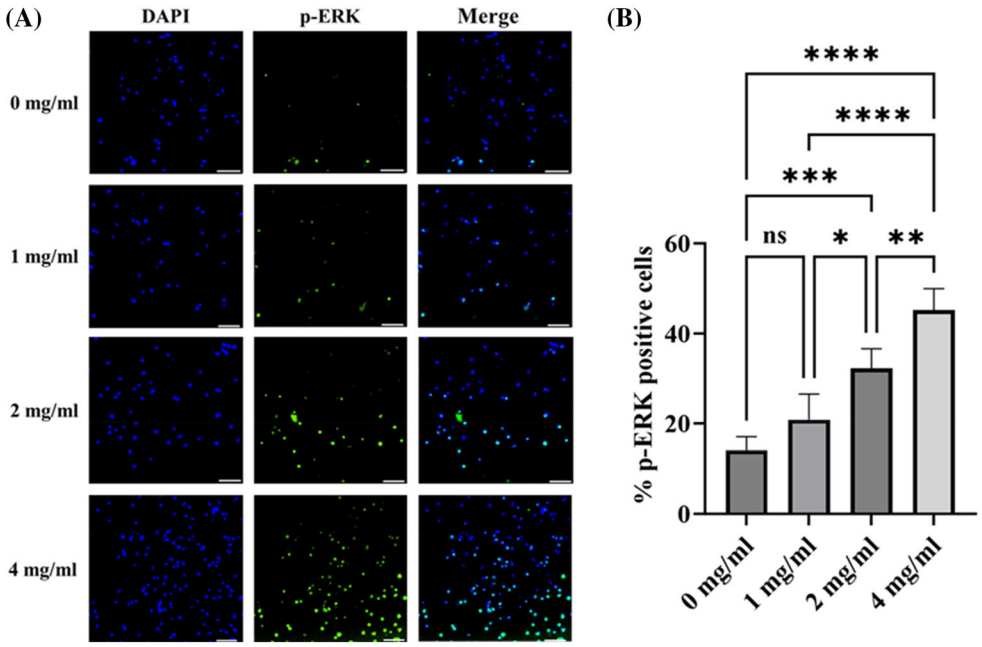


**FIGURE 3** Percentage of p-ERK positive cells increases with an increase in applied RGD concentration. (A) Representative fluorescence microscopy images of p-ERK staining on day 5 of MDA-MB-231Br cells, blue—DAPI (nucleus), green—p-ERK. (B) Quantification of p-ERK positive MDA-MB-231Br cells cultured on HA hydrogels functionalized with various concentrations of RGD. Error bars represent standard deviation. Scale bar = 100 μm. $N \geq 4$ replicates per condition. Statistically significant difference indicator via Brown-Forsythe ANOVA followed by Tukey-HSD test: (*$p < .05$; **$p < .01$; ***$p < .001$; ****$p < .0001$).

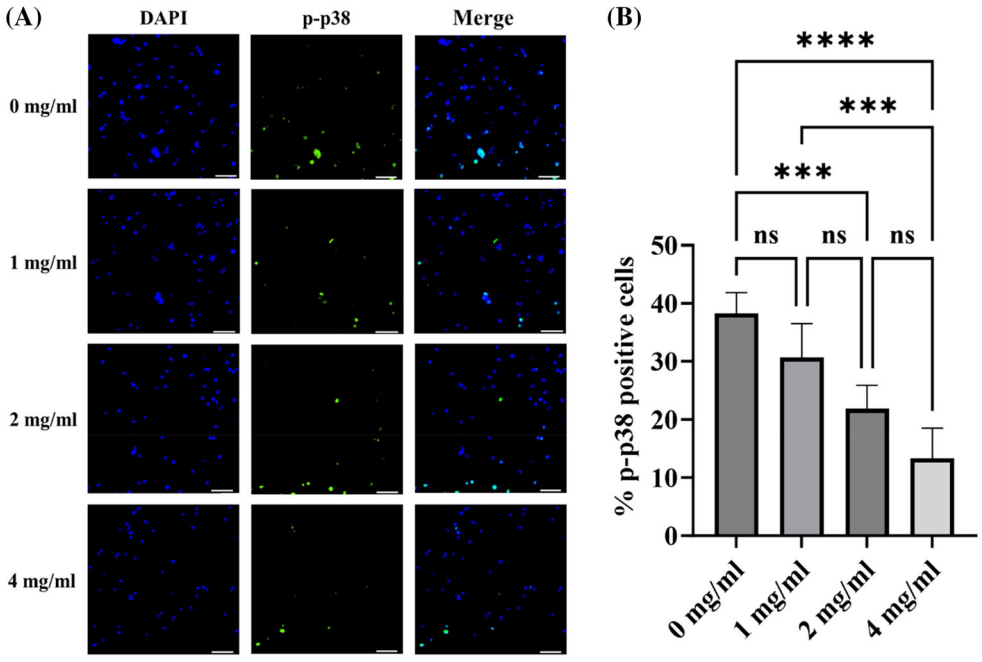


**FIGURE 4** Percentage of p-p38 positive cells decreases with an increase in applied RGD concentration. (A) Representative fluorescence microscopy images of p-p38 staining on day 5 of MDA-MB-231Br cells, blue—DAPI (nucleus), green—p-p38. (B) Quantification of p-p38 positive MDA-MB-231Br cells cultured on HA hydrogels functionalized with various concentrations of RGD. Error bars represent standard deviation. Scale bar = 100 μm. $N \geq 4$ replicates per condition. Statistically significant difference indicator via Brown-Forsythe ANOVA followed by Tukey-HSD test (***$p < .001$; ****$p < .0001$).

**TABLE 2** Ratio of percentage of p-ERK positive cells to p-p38 positive cells as a function of applied RGD concentration.

| Applied RGD concentration (mg/mL) | Ratio of %p-ERK+ to %p-p38+ cells |
|---|---|
| 0 | 0.37 |
| 1 | 0.68 |
| 2 | 1.47 |
| 4 | 3.39 |

(Figure 3). The expression levels for p-p38 exhibited an opposite trend, as noted for p-ERK with varying RGD concentration. In particular, %p-p38 positivity decreased with an increase in RGD concentration applied to the HA hydrogels. The percentage of p-p38 positive cells of RGD-free HA hydrogels was 38.3% ± 3.6%, but this value dropped to 30.7% ± 5.8%, 21.9% ± 4.0%, and 13.3% ± 5.2% for conditions with applied RGD concentration of 1, 2, and 4 mg/mL, respectively (Figure 4).

We also quantified the ratio of % p-ERK positive cells to %p-p38 positive cells as a function of RGD concentration. We found that the ratio increased with an increase in RGD concentration with ratios greater than 1 observed in hydrogels with 2 and 4 mg/mL applied RGD concentration (Table 2). These results were also confirmed via mean intensity measurements (Figures S4 and S5, Table S1). Overall, these results indicated that cells in the absence of RGD or 1 mg/mL applied RGD concentration exhibited a dormant phenotype, whereas cells cultured in the presence of 2 or 4 mg/mL applied RGD concentration exhibited a proliferative phenotype.

### 3.5 | Reversibility of the induced dormant phenotype

We next investigated if the observed dormant phenotype was reversible. For this study, we seeded 10,000 MDA-MB-231Br cells on HA hydrogels without RGD and cultured them for 5 days. We then retrieved the cells and transferred them to newly fabricated HA hydrogels that were functionalized with 0 or 4 mg/mL RGD solution and cultured them for an additional 5 days.

Upon transfer to the RGD-deficient hydrogel, the cells exhibited a rounded morphology with minimal cell spreading and an average cell spreading of 300 ± 95 $\mu m^2$. However, when the cells were transferred to the RGD-enriched hydrogel, we observed a shift from dormant to proliferative state, as evidenced by a spindle-like cell morphology and increased cell spreading. The average cell spreading area for this condition was 541 ± 342 $\mu m^2$ and significantly higher than that observed in RGD-deficient hydrogel at day 10 (Figure 5).

These findings were further corroborated through the EdU staining (Figure 6). When cells were transferred and cultured on RGD-enriched hydrogel for a duration of 10 days, the percentage of EdU positive cells was found to be 25% ± 6%, which was significantly higher than that observed in the RGD-deficient hydrogels (11% ± 7%) indicating that the cells adopted a proliferative state upon transfer to RGD-enriched hydrogel. Overall, these results demonstrate that the observed dormant phenotype was reversible, and that varying the RGD concentration influences dormancy versus proliferation in brain metastatic breast cancer cells.

### 3.6 | Involvement of β1 integrin in mediating cell phenotype

To investigate the mechanism involved in mediating cell phenotype, we tested integrin β1 due to its significance in various cellular processes, including cell adhesion, signaling, and interactions with the extracellular matrix (ECM).[35–37] Specifically, we performed blocking studies for integrin β1 in HA hydrogels functionalized with 4 mg/mL applied RGD concentration, as this condition promoted the highest cell spreading and proliferation compared to other conditions (Figures 1 and 2). We found that the average cell spreading area was 1014 ± 237 $\mu m^2$ without integrin β1 blocking, which was significantly reduced to 553 ± 211 $\mu m^2$ with integrin β1 blocking at day 5 (Figure 7). Similarly, we found that the percentage of EdU positive cells was 43% ± 7% without integrin β1 blocking, which was significantly reduced to 35% ± 6% with integrin β1 blocking at day 5 (Figure 7). These results indicated that β1 integrin, partly mediated cell spreading and cell proliferation in our hydrogel platform.

To further assess the involvement of β1 integrin in the dormant-to-proliferative switch, we performed blocking studies for integrin β1 in transferred cells on HA hydrogels functionalized with 4 mg/mL applied RGD concentration. We found that the average cell spreading area was 1275 ± 380 $\mu m^2$ without integrin β1 blocking, which was significantly reduced to 883 ± 330 $\mu m^2$ with integrin β1 blocking at day 12 (Figure S6). Similarly, we found that the percentage of EdU positive cells was 56% ± 7% without integrin β1 blocking, which was significantly reduced to 41% ± 6% with integrin β1 blocking at day 12 (Figure S6). These results indicated that β1 integrin, partly mediated spreading and proliferation in cells that transitioned to a proliferative state from a dormant state in our hydrogel platform.

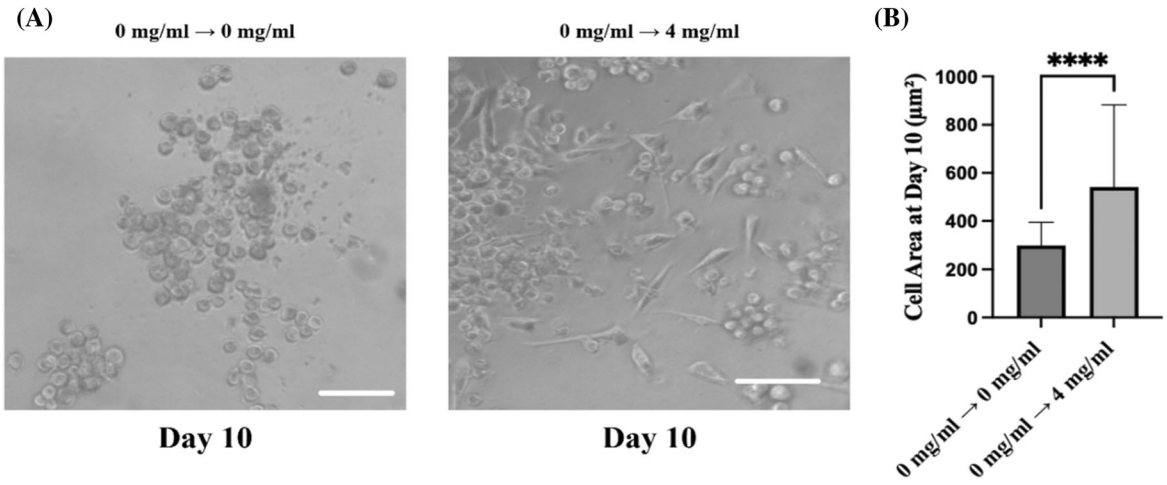


**FIGURE 5** MDA-MB-231Br cells exhibited a higher level of cell spreading at day 10 in HA hydrogels containing 4 mg/mL applied RGD concentration (0 mg/mL → 4 mg/mL) compared to hydrogels without RGD (0 mg/mL → 0 mg/mL) post transfer from HA hydrogels without RGD at day 5. (A) Bright field images of MDA-MB-231Br cells transferred from HA hydrogels without RGD to HA hydrogels without RGD (0 mg/mL → 0 mg/mL) or 4 mg/mL applied RGD concentration (0 mg/mL → 4 mg/mL) taken at day 10 (5 days post transfer). (B) Quantification of cell spreading area post transfer at day 10. Error bars represent standard deviation. Scale bar = 100 μm. $N \geq 4$ replicates per condition. Statistically significant difference indicator via Student's *t*-test (****$p < .0001$).

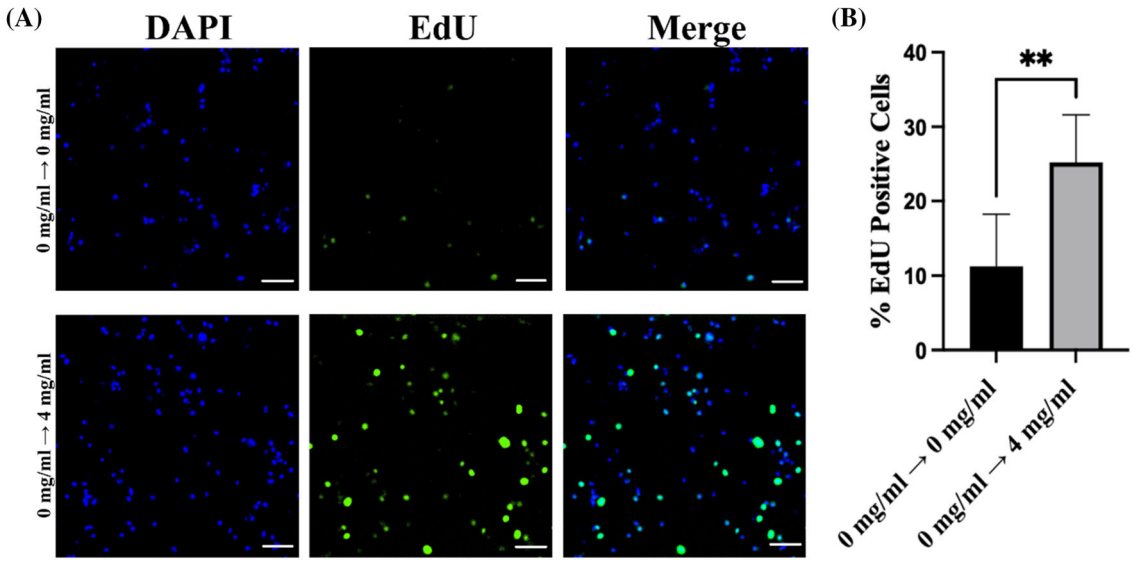


**FIGURE 6** MDA-MB-231Br cells expressed a higher percentage of EdU positivity at day 10 in HA hydrogels containing 4 mg/mL applied RGD concentration (0 mg/mL → 4 mg/mL) compared to hydrogels without RGD (0 mg/mL → 0 mg/mL) post transfer from HA hydrogels without RGD at day 5. (A) Representative fluorescence microscopy images of EdU staining on day 10 of MDA-MB-231Br cells. (B) Quantification of EdU positive MDA-MB-231Br cells post transfer. $N \geq 3$ replicates per condition. Error bars represent standard deviation. Scale bar = 100 μm. Statistically significant difference indicator via Student's *t*-test (**$p < .01$).

## 4 | DISCUSSION

In this study, we investigated the impact of varying RGD concentration on the regulation of dormancy versus proliferation in brain metastatic breast cancer cells in a biomimetic HA hydrogel in vitro. Varying the RGD concentration provided varying levels of adhesivity and allowed us to examine how such environments may impact tumor cell dormancy. Generally, studies investigating the role of biophysical or biochemical cues in regulating dormancy in the context of BCBM have been limited.[22,25,27–29] To this end, our group previously examined the impact of biophysical cues and how it regulates dormancy in brain metastatic breast cancer cells in a biomimetic HA hydrogel.[22] However, the impact of biochemical cues (e.g., varying levels of cell adhesivity) was not tested. Our study bridges this gap by demonstrating that varying the RGD concentration in a biomimetic HA hydrogel influences dormancy vs. proliferation in brain metastatic breast cancer cells.

The brain microenvironment plays an important role in regulating the fate of brain metastatic breast cancer cells. However, how various cues presented by the microenvironment influence the regulation of dormancy remain poorly understood. This is, in part, due to the lack of relevant biomimetic model systems that provide controllable environments and allow for the investigation of various microenvironmental cues involved in dormancy as well as the dormant-to-proliferative switch. As such, our study provides an important step in addressing this need and demonstrates the role of biochemical cues in regulating dormancy as well as the dormant-to-proliferative switch by employing biomimetic HA hydrogels functionalized with the integrin binding RGD peptide derived from fibronectin/vitronectin, ECM proteins present in the brain environment.[16,38]

Our findings reveal a direct correlation between the applied RGD concentration on HA hydrogels and cell spreading in brain metastatic breast cancer cells. These results are consistent with previous studies on other cancer types, which have also demonstrated a similar response to increasing RGD concentration in their respective microenvironments.[39–42] We also found a significant increase in cell proliferation on HA hydrogel functionalized with a higher concentration of RGD peptides. This observation can be attributed to the interaction between the RGD peptide and integrin receptors present on the surface of MDA-MB-231Br cells. These interactions are known to activate downstream signaling pathways that promote cell proliferation.[43]

Previous work has shown that dormant cancer cells have low levels of p-ERK and high levels of p-p38.[11,44] In addition, low ratio of p-ERK to p-p38 positivity has been reported to be an indicator of dormancy.[34] Our study findings revealed that an increase in functionalized RGD motifs on the HA hydrogel led to a substantial increase in the p-ERK/p-p38 ratio, indicating that cells adopted a proliferative state. In contrast, in the absence of RGD or lower applied RGD concentration (i.e., 1 mg/mL) cells adopted a dormant state. These findings further demonstrate that the biochemical cues can be independently tuned to study dormancy versus proliferation in vitro. Our findings are also consistent with prior work that investigated the impact of RGD peptide presence in a three-dimensional PEG-based hydrogel on the growth and dormancy of BrM2a-831 cells (a brain-seeking variant of the MDA-MB-231 parental cell line).[29] These variants differ in the selection process used to create the variant and the adaptations that occurred during propagation.

Reawakening of dormant tumor cells contributes to disease relapse at metastatic sites.[45–47] Recent studies suggest that the activation of

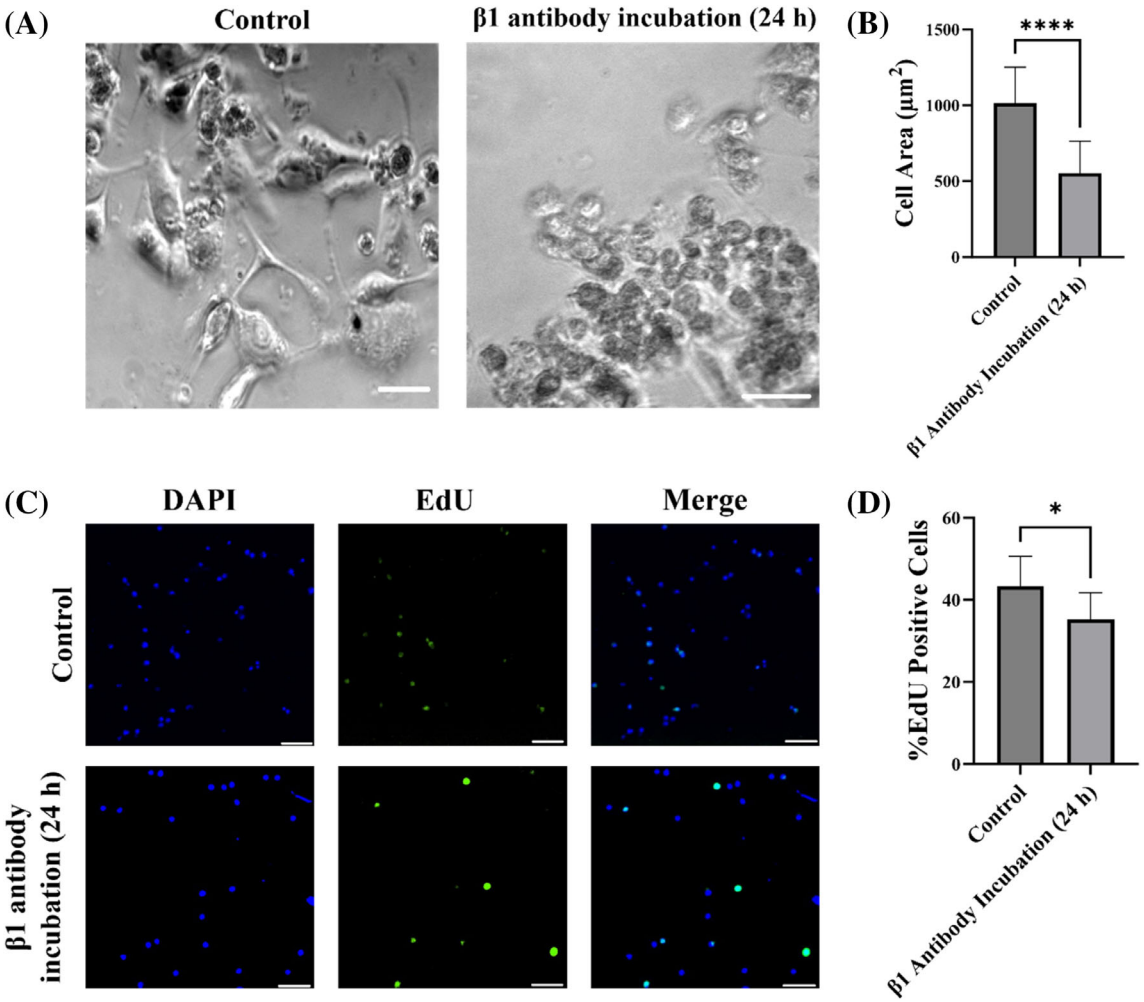


**FIGURE 7** Cell spreading area and proliferation of MDA-MB-231Br cells cultured in the presence of 4 mg/mL applied RGD concentration is decreased by incubating the cells for 24 h with 2 μg/mL integrin β1 antibody. (A) Bright field images of day 5 of 10 k MDA-MB-231Br single cells seeded on HA hydrogels. (B) Quantification of cell spreading area on HA hydrogels functionalized with 4 mg/mL RGD after 24 h of incubation with and without integrin β1 antibody (control). (C) Representative fluorescence microscopy images of EdU staining on day 5 of MDA-MB-231Br cells. (D) Quantification of EdU-positive MDA-MB-231Br cells cultured on HA hydrogels functionalized with 4 mg/mL RGD after 24 h of incubation with and without integrin β1 antibody (control). Error bars represent standard deviations. Scale bar = 50 μm for A and scale bar = 100 μm for C. $N \geq 5$ replicates per condition. Statistically significant difference indicator via Student's *t*-test (*$p < .05$; ****$p < .0001$).

dormant cells is dependent on specific cues provided by the microenvironment, and that the ECM plays a crucial role in the reawakening process.[48–51] Specifically, alterations in the ECM composition or signaling molecules have the potential to induce the reactivation of dormant cancer cells.[52–55] For example, changes in the level of specific matrix proteins (i.e., Collagen-I) can stimulate the proliferation of previously dormant mouse mammary cancer cells.[56] In our study, we found that after being transferred from RGD-free HA hydrogels to hydrogels with the highest RGD concentration, MDA-MB-231Br cells exhibited a significant increase in both cell spreading area and proliferation 5 days post transfer. However, the levels of cell spreading, and proliferation were lower than that observed for cells directly cultured on hydrogels with 4 mg/mL applied RGD concentration (Figures 5 and 6 vs. Figures 1 and 2). This could be attributed to the dormancy period which was absent for cells directly cultured on hydrogels with 4 mg/mL applied RGD concentration. To understand the associated mechanism, we performed integrin β1 blocking studies. We found that when β1 integrin was blocked, there was a significant reduction in cell spreading area and the percentage of proliferating cells. Moreover, in cells transitioning from a dormant to a proliferative state, we observed similar results, underscoring the involvement of β1 integrin in mediating cell phenotypes. Taken together, our results demonstrate that the dormant phenotype can be reversed by manipulating the RGD concentration in their microenvironment and that the interaction with RGD (via β1 integrin) plays a crucial role in the reactivation of dormant cancer cells. These findings also emphasize the importance of understanding the role of the microenvironment in the reawakening of dormant cancer cells, which is critical for developing new therapeutic strategies to prevent disease relapse.

In sum, we have shown that varying the RGD concentration on a HA hydrogel influences dormancy vs. proliferation and also plays a role

in the dormant-to-proliferative switch, mediated, in part, via β1 integrins. However, we note the following limitations of the work: (1) This work has not investigated cancer cell invasion or metastatic potential as a function of RGD concentration and would be topic of future studies. (2) Future studies would also examine how RGD density influences dormancy vs. proliferation in tumor cells encapsulated in 3D hydrogels. (3) Future studies would expand testing with additional cell types, including non-invasive cancer cells, as well as patient-derived cancer cells to understand tumor heterogeneity. (4) In future work, we will examine the impact of other ECM derived peptides, such as Laminin- and Collagen-derived peptides on dormancy versus proliferation.

## 5 | CONCLUSIONS

In this study, we report the impact of RGD peptide concentration in regulating dormancy versus proliferation in brain metastatic breast cancer cells in a biomimetic HA hydrogel. An increase in RGD concentration resulted in enhanced cell spreading with cells transitioning from a rounded morphology in the absence of RGD or lower applied RGD concentration (1 mg/mL) to adopting a spindle-like morphology at higher applied RGD concentration (i.e., 2 or 4 mg/mL). An increase in RGD concentration resulted in an increase in cell proliferation. The ratio of p-ERK to p-p38 positivity was significantly lower in hydrogels without RGD and in hydrogels with lower applied RGD concentration compared to the hydrogels functionalized with higher RGD concentration further indicative of cellular dormancy versus proliferation. We also demonstrated that the HA hydrogel-induced cellular dormancy was reversible via modulation of the culture environment. Finally, we demonstrated the involvement of β1 integrin in mediating cell phenotype in the HA hydrogel platform. Overall, the HA hydrogel-based platform could be used to investigate the impact of several biochemical cues (proteins or peptides) on the regulation of dormancy in brain metastatic breast cancer cells in vitro.

### ACKNOWLEDGMENTS

The authors acknowledge financial support from the National Science Foundation (CBET 1749837, to S.R.) and the Alabama EPSCoR Graduate Research Fellowship (to K.G.).

### CONFLICT OF INTEREST STATEMENT

The authors declare no conflict of interest.

### DATA AVAILABILITY STATEMENT

The data that support the findings of this study are available from the corresponding author upon reasonable request.

### ORCID

*Shreyas S. Rao* https://orcid.org/0000-0001-7649-0171

### REFERENCES

1. McGuire S. World cancer report 2014. Geneva, Switzerland: World Health Organization, international agency for research on cancer, WHO Press, 2015. *Adv Nutr*. 2016;7(2):418-419.
2. Sun Y-S, Zhao Z, Yang Z-N, et al. Risk factors and preventions of breast cancer. *Int J Biol Sci*. 2017;13(11):1387-1397.
3. Arnold M, Morgan E, Rumgay H, et al. Current and future burden of breast cancer: global statistics for 2020 and 2040. *Breast*. 2022;66:15-23.
4. Heer E, Harper A, Escandor N, Sung H, McCormack V, Fidler-Benaoudia MM. Global burden and trends in premenopausal and postmenopausal breast cancer: a population-based study. *Lancet Glob Health*. 2020;8(8):e1027-e1037.
5. Hosonaga M, Saya H, Arima Y. Molecular and cellular mechanisms underlying brain metastasis of breast cancer. *Cancer Metastasis Rev*. 2020;39:711-720.
6. Bailleux C, Eberst L, Bachelot T. Treatment strategies for breast cancer brain metastases. *Br J Cancer*. 2021;124(1):142-155.
7. Corti C, Antonarelli G, Criscitiello C, et al. Targeting brain metastases in breast cancer. *Cancer Treat Rev*. 2022;103:102324.
8. Aguirre-Ghiso JA. Models, mechanisms and clinical evidence for cancer dormancy. *Nat Rev Cancer*. 2007;7(11):834-846.
9. Giancotti FG. Mechanisms governing metastatic dormancy and reactivation. *Cell*. 2013;155(4):750-764.
10. Dittmer J. Mechanisms governing metastatic dormancy in breast cancer. *Semin Cancer Biol*. 2017;44:72-82.
11. Park S-Y, Nam J-S. The force awakens: metastatic dormant cancer cells. *Exp Mol Med*. 2020;52(4):569-581.
12. Paget S. The distribution of secondary growths in cancer of the breast. *Lancet*. 1889;133(3421):571-573.
13. Fidler IJ. The pathogenesis of cancer metastasis: the 'seed and soil' hypothesis revisited. *Nat Rev Cancer*. 2003;3(6):453-458.
14. Rao SS, Kondapaneni RV, Narkhede AA. Bioengineered models to study tumor dormancy. *J Biol Eng*. 2019;13:1-12.
15. Goodarzi K, Rao SS. Hyaluronic acid-based hydrogels to study cancer cell behaviors. *J Mater Chem B*. 2021;9(31):6103-6115.
16. Chintala SK, Rao JS. Invasion of human glioma: role of extracellular matrix proteins. *Front Biosci-Landmark*. 1996;1(4):324-339.
17. Fang JY, Tan S-J, Wu Y-C, Yang Z, Hoang BX, Han B. From competency to dormancy: a 3D model to study cancer cells and drug responsiveness. *J Transl Med*. 2016;14(1):38.
18. Barkan D, Green JE. An in vitro system to study tumor dormancy and the switch to metastatic growth. *JoVE*. 2011;54:e2914.
19. Liu Y, Lv J, Liang X, et al. Fibrin stiffness mediates dormancy of tumor-repopulating cells via a Cdc42-driven Tet2 epigenetic program. *Cancer Res*. 2018;78(14):3926-3937.
20. Pradhan S, Slater JH. Tunable hydrogels for controlling phenotypic cancer cell states to model breast cancer dormancy and reactivation. *Biomaterials*. 2019;215:119177.
21. Farino CJ, Pradhan S, Slater JH. The influence of matrix-induced dormancy on metastatic breast cancer chemoresistance. *ACS Appl Bio Mater*. 2020;3(9):5832-5844.
22. Narkhede AA, Crenshaw JH, Crossman DK, Shevde LA, Rao SS. An in vitro hyaluronic acid hydrogel based platform to model dormancy in brain metastatic breast cancer cells. *Acta Biomater*. 2020;107:65-77.
23. Narkhede AA, Crenshaw JH, Manning RM, Rao SS. The influence of matrix stiffness on the behavior of brain metastatic breast cancer cells in a biomimetic hyaluronic acid hydrogel platform. *J Biomed Mater Res A*. 2018;106(7):1832-1841.
24. Nakod PS, Kondapaneni RV, Edney B, Kim Y, Rao SS. The impact of temozolomide and lonafarnib on the stemness marker expression of glioblastoma cells in multicellular spheroids. *Biotechnol Prog*. 2022;38(5):e3284.
25. Kondapaneni RV, Rao SS. Matrix stiffness and cluster size collectively regulate dormancy versus proliferation in brain metastatic breast cancer cell clusters. *Biomater Sci*. 2020;8(23):6637-6646.
26. Nakod PS, Kim Y, Rao SS. Three-dimensional biomimetic hyaluronic acid hydrogels to investigate glioblastoma stem cell behaviors. *Biotechnol Bioeng*. 2020;117(2):511-522.

27. Kondapaneni RV, Shevde LA, Rao SS. A biomimetic hyaluronic acid hydrogel models mass dormancy in brain metastatic breast cancer spheroids. *Adv Biol*. 2023;7(1):2200114.
28. Kondapaneni RV, Warren R, Rao SS. Low dose chemotherapy induces a dormant state in brain metastatic breast cancer spheroids. *AICHE J*. 2022;68(12):e17858.
29. Farino Reyes CJ, Pradhan S, Slater JH. The influence of ligand density and degradability on hydrogel induced breast cancer dormancy and reactivation. *Adv Healthc Mater*. 2021;10(11):2002227.
30. Buck SB, Bradford J, Gee KR, Agnew BJ, Clarke ST, Salic A. Detection of S-phase cell cycle progression using 5-ethynyl-2′-deoxyuridine incorporation with click chemistry, an alternative to using 5-bromo-2′-deoxyuridine antibodies. *Biotechniques*. 2008;44(7):927-929.
31. Lovitt CJ, Hilko DH, Avery VM, Poulsen S-A. Development of ethynyl-2′-deoxyuridine chemical probes for cell proliferation. *Bioorg Med Chem*. 2016;24(18):4272-4280.
32. Wagner EF, Nebreda ÁR. Signal integration by JNK and p38 MAPK pathways in cancer development. *Nat Rev Cancer*. 2009;9(8):537-549.
33. Hui L, Bakiri L, Stepniak E, Wagner EF. p38&alpha: a suppressor of cell proliferation and tumorigenesis. *Cell Cycle*. 2007;6(20):2429-2433.
34. Aguirre-Ghiso JA, Estrada Y, Liu D, Ossowski L. ERKMAPK activity as a determinant of tumor growth and dormancy; regulation by p38SAPK1. *Cancer Res*. 2003;63(7):1684-1695.
35. Adelsman MA, McCarthy JB, Shimizu Y. Stimulation of β1-integrin function by epidermal growth factor and Heregulin-β has distinct requirements for erbB2 but a similar dependence on phosphoinositide 3-OH kinase. *Mol Biol Cell*. 1999;10(9):2861-2878.
36. Felding-Habermann B. Integrin adhesion receptors in tumor metastasis. *Clin Exp Metastasis*. 2003;20(3):203-213.
37. Bachmann M, Kukkurainen S, Hytönen VP, Wehrle-Haller B. Cell adhesion by integrins. *Physiol Rev*. 2019;99(4):1655-1699.
38. Chakraborty K. Different Role of Extracellular Matrix (ECM) in Brain. Available at SSRN 3839969 2021. 2021.
39. Balion Z, Sipailaite E, Stasyte G, et al. Investigation of cancer cell migration and proliferation on synthetic extracellular matrix peptide hydrogels. *Front Bioeng Biotechnol*. 2020;8:8.
40. Aldana AA, Morgan FLC, Houben S, Pitet LM, Moroni L, Baker MB. Biomimetic double network hydrogels: combining dynamic and static crosslinks to enable biofabrication and control cell-matrix interactions. *J Polym Sci*. 2021;59(22):2832-2843.
41. Zhou N, Ma X, Hu W, Ren P, Zhao Y, Zhang T. Effect of RGD content in poly(ethylene glycol)-crosslinked poly(methyl vinyl ether-alt-maleic acid) hydrogels on the expansion of ovarian cancer stem-like cells. *Mater Sci Eng C*. 2021;118:111477.
42. Zustiak SP, Dadhwal S, Medina C, et al. Three-dimensional matrix stiffness and adhesive ligands affect cancer cell response to toxins. *Biotechnol Bioeng*. 2016;113(2):443-452.
43. Nieberler M, Reuning U, Reichart F, et al. Exploring the role of RGD-recognizing integrins in cancer. *Cancer*. 2017;9(9):116.
44. Sosa MS, Avivar-Valderas A, Bragado P, Wen H-C, Aguirre-Ghiso JA. ERK1/2 and p38α/β signaling in tumor cell quiescence: opportunities to control dormant residual disease. *Clin Cancer Res*. 2011;17(18):5850-5857.
45. Valastyan S, Weinberg RA. Tumor metastasis: molecular insights and evolving paradigms. *Cell*. 2011;147(2):275-292.
46. Nguyen DX, Bos PD, Massagué J. Metastasis: from dissemination to organ-specific colonization. *Nat Rev Cancer*. 2009;9(4):274-284.
47. Pradhan S, Sperduto JL, Farino CJ, Slater JH. Engineered in vitro models of tumor dormancy and reactivation. *J Biol Eng*. 2018;12:1-19.
48. Joyce JA, Pollard JW. Microenvironmental regulation of metastasis. *Nat Rev Cancer*. 2009;9(4):239-252.
49. Deepak K, Vempati R, Nagaraju GP, et al. Tumor microenvironment: challenges and opportunities in targeting metastasis of triple negative breast cancer. *Pharmacol Res*. 2020;153:104683.
50. Sistigu A, Musella M, Galassi C, Vitale I, De Maria R. Tuning cancer fate: tumor microenvironment's role in cancer stem cell quiescence and reawakening. *Front Immunol*. 2020;11:2166.
51. Linde N, Fluegen G, Aguirre-Ghiso J. The relationship between dormant cancer cells and their microenvironment. *Adv Cancer Res*. 2016;132:45-71.
52. Grandhi TSP, Potta T, Nitiyanandan R, Deshpande I, Rege K. Chemo-mechanically engineered 3D organotypic platforms of bladder cancer dormancy and reactivation. *Biomaterials*. 2017;142:171-185.
53. Di Martino JS, Akhter T, Bravo-Cordero JJ. Remodeling the ECM: implications for metastasis and tumor dormancy. *Cancer*. 2021;13(19):4916.
54. Parker AL, Cox TR. The role of the ECM in lung cancer dormancy and outgrowth. *Front Oncol*. 2020;10:1766.
55. Sosa MS, Bragado P, Aguirre-Ghiso JA. Mechanisms of disseminated cancer cell dormancy: an awakening field. *Nat Rev Cancer*. 2014;14(9):611-622.
56. Barkan D, El Touny LH, Michalowski AM, et al. Metastatic growth from dormant cells induced by a col-I—enriched fibrotic environment metastatic outgrowth from dormant tumor cells. *Cancer Res*. 2010;70(14):5706-5716.


## SUPPORTING INFORMATION

Additional supporting information can be found online in the Supporting Information section at the end of this article.

**How to cite this article:** Goodarzi K, Lane R, Rao SS. Varying the RGD concentration on a hyaluronic acid hydrogel influences dormancy versus proliferation in brain metastatic breast cancer cells. *J Biomed Mater Res*. 2024;112(5):710-720. doi:10.1002/jbm.a.37651